

# Electrocardiogram synthesis from Two asynchronous leads to Ten leads

Yong-Yeon Jo, Joon-Myoung Kwon

yy.jo,cto@medicalai.com

MedicalAI Co., Ltd.

Seoul, South Korea

## ABSTRACT

The electrocardiogram (ECG) records electrical signals in a non-invasive way to observe the condition of the heart, typically looking at the heart from 12 different directions. Several types of the cardiac disease are diagnosed by using 12-lead ECGs. Recently, various wearable devices have enabled immediate access to the ECG without the use of bulky equipment. However, they only provide ECGs with a couple of leads. This results in an inaccurate diagnosis of cardiac disease due to lacking of required leads. We propose a deep generative model for ECG synthesis from two asynchronous leads to ten leads. It first represents a heart condition referring to two leads, and then generates ten leads based on the represented heart condition. Both the rhythm and amplitude of leads generated resemble those of the original ones, while the technique removes noise and the baseline wander appearing in the original leads. As a data augmentation method, our model improves the classification performance of models compared with models using ECGs with only one or two leads.

## CCS CONCEPTS

• **Applied computing** → *Life and medical sciences*; • **Computing methodologies** → *Artificial intelligence*.

## KEYWORDS

Electrocardiogram; Synthesis; Generative model; Signal-to-signal translation

### ACM Reference Format:

Yong-Yeon Jo, Joon-Myoung Kwon. 2018. Electrocardiogram synthesis from Two asynchronous leads to Ten leads. In . ACM, New York, NY, USA, 10 pages. <https://doi.org/10.1145/1122445.1122456>

## 1 INTRODUCTION

An electrocardiogram (ECG) records the electrical signals generated by the heart by using external electrodes, which is a painless and non-invasive way to help diagnose many heart conditions [21, 33]. A standard ECG consists of 12 leads, looking at the heart from various angles. There are six limb leads and six precordial leads. The limb leads (Lead I, Lead II, Lead III, aVR, aVL, and aVF) record

signals of the heart at the arms and/or legs, while the precordial leads (V1~6) are placed on the chest, and record anteriorly directed electrical activity. The limb and precordial leads are mutually orthogonal. Recently, there have been several studies on deep learning models using ECGs to support the diagnosis of cardiac diseases such as atrial fibrillation [4, 13], heart failure with preserved ejection fraction [24], myocardial infarction [1, 6], and hypertrophic cardiomyopathy [22].

With the advancement of smart devices, various wearable ones have appeared and enabled measure ECGs immediately anywhere [17, 29, 32, 38]. Though these devices provide ECGs with only a couple of leads [5], a missing of particular signals by insufficient leads could degrade diagnostic capabilities, compared with the standard 12-lead ECG taken using medical equipment. The existing literature also shows that insufficient leads cause the performance of deep learning models in diagnosing diseases [9, 23].

A study reported that a wearable device could measure more than a single lead with different postures, though measured leads are recorded asynchronously [36]. Because a lead implies a heart condition projected for the vector representing the magnitude and direction of electrical signals at any particular axis, a 12-lead ECG is conjectured from given some leads. With the assumption of the circumstance that given at least two asynchronous leads, we propose a deep generative model for the ECG synthesis from given leads to ten leads, and we named this model ECGT2T.

For ECGT2T, we adopt the concept of image-to-image translation models based on a generative adversarial network (GAN) [10, 19, 42], which translates a source image to another image depicting the style of a reference image. ECGT2T first represents the cardiac condition referring to two given leads and learn the lead styles corresponding to their cardiac condition. It generates a lead referring to its corresponding style with any given single lead.

The architecture consists of four networks. The style network represents a cardiac condition from two asynchronous leads and captures ten styles for other respective leads. The mapping network only produces ten styles from a random variable, which helps to enhance the capability of the depiction for cardiac styles in the style network. The generative network generates a lead from any single input lead with a cardiac style. The discriminative network distinguishes between original and generated leads as widely used typical GAN.

To evaluate the quality for generated leads and the availability of ECGT2T, we obtained two ECG datasets collected at the Physikalisch Technische Bundesanstalt (PTB-XL) [37] and Chapman University and Shaoxing People's Hospital (CUSPH) [40], respectively. We train ECGT2T using only training samples in the PTB-XL dataset. To clarify the necessity for at least two leads in

Permission to make digital or hard copies of all or part of this work for personal or classroom use is granted without fee provided that copies are not made or distributed for profit or commercial advantage and that copies bear this notice and the full citation on the first page. Copyrights for components of this work owned by others than ACM must be honored. Abstracting with credit is permitted. To copy otherwise, or republish, to post on servers or to redistribute to lists, requires prior specific permission and/or a fee. Request permissions from [permissions@acm.org](mailto:permissions@acm.org).

© 2018 Association for Computing Machinery.  
ACM ISBN 978-1-4503-XXXX-X/18/06...\$15.00  
<https://doi.org/10.1145/1122445.1122456>

ECGT2T, we developed another model for the ECG synthesis from a single lead to the other 11 leads (ECGS2E).

As the first assessment for the synthetic quality, we compared the rhythm and amplitude between synthesized and original leads. The R peak is one of the most important wave points in ECG. We found the errors for the timing and amplitude were less than under 15ms and about 10%, respectively. In addition, we checked out the quality by visually comparing original and generative leads. ECGT2T generates leads nearly equivalent to the original one, while it removes artifacts such as noise and baseline wandering that result in inaccurate and misleading clinical interpretation [7].

To verify the applicability, we used ECGT2T as a lead augmentation method to construct a standard 12-lead ECG from two asynchronous leads. We constructed six evaluation sets with different lead combinations: single-lead, two synchronous-lead, two asynchronous-lead, 12-lead by ECGS2E, 12-lead by ECGT2T, and original 12-lead sets. We also develop a classifier based on ResNet [14] to classify heart diseases. As a result, the classifier trained using the 12-lead ECG set augmented by ECGT2T outperforms others in all metrics, except for one using the original 12-lead ECG set. We expect that this result implies that the wearable devices could be utilized to diagnose cardiac diseases, though they provide insufficient leads.

Our contribution is as follows.

- We proposed the electrocardiogram synthesis based on GAN from two asynchronous leads to ten leads to construct the standard 12-lead ECG, called ECGT2T.
- We access the synthetic quality. We showed that both the rhythm and amplitude on leads generated by ECGT2T closely resemble those of the original ones. We also identified that ECGT2T removes artifacts such as noise and baseline fluctuations appearing in the original leads.
- We validated the applicability of ECGT2T by using it as a data augmentation method. The classifier trained by the augmented ECG set outperforms those by the ECG sets composed with partial leads.

The organization of the paper is as follows. Section 2 introduces the related work. Section 3 briefly introduces the electrocardiogram and describes the problem definition and proposed methods. Section 4 analyzes the generation performance and validates the applicability as a lead augmentation method. Finally, Section 5 summarizes and concludes the paper.

## 2 RELATED WORK

We introduce the basic concept of the generative adversarial network (GAN), studies for application in the electrocardiogram (ECG), and image-to-image translation models to which we refer.

### 2.1 Generative adversarial network

GAN is a generative model to generate data from scratch. It is composed of two networks: a generative network  $G$  and a discriminative network  $D$ .  $G$  is trained to learn the distribution of the original data and to generate fake data that is likely to be in the real world when a random variable is given. Adversely,  $D$  is trained to distinguish between real-world data and fake data constructed by  $G$ . The objective function for GAN is as follows:  $G$  learns so

that the objective function becomes the minimum, and  $D$  learns the maximum. Finally, at convergence of the zero-sum game between  $G$  and  $D$ ,  $G$  can be utilized to make synthetic data.

$$\min_G \max_D V(D, G) = \mathbb{E}_{x \sim p_{data}(x)} [\log D(x)] + \mathbb{E}_{z \sim p_x(z)} [\log(1 - D(G(z)))]$$

### 2.2 Generative adversarial network for electrocardiogram

Many researches attempt to apply GAN to the electrocardiogram. Fei Zhu et. al. [41] proposed GAN based on the bidirectional long short-term memory (LSTM) with convolutional neural network (CNN), and showed that the model was better than other models such as auto-encoder and variational auto-encoder. This model only provides the facility to generate a single lead from a latent code.

Naren Wulan et. al. [39] proposed GAN to synthesize the signals using the short-term Fourier transform and stationary wavelet transform. The model could change a signal to three different heart-beat types, instead of the signal in other leads to be required to diagnose cardiac diseases. Tomer Golany et. al. [12] suggested a model for synthesizing ECG beats based on LSTM-GAN. Its model augments the training dataset with various types of heart beats. Those models help to alleviate the unbalanced label problem in the train dataset. Those models help to alleviate the unbalanced label problem in the train dataset.

Eoin Brophy [8] proposed the multivariate GAN that generates V5 from Lead II. This showed the possibility of generating another lead from a single lead. In addition, some GANs are developed for denosing the ECG [3, 11].

### 2.3 Image-to-image translation

Recently, image-to-image translation has been actively studied using the deep generative models.

Pix2Pix [16] triggers the image-to-image translation studies. It translates an image by learning the paired data of the original and the target images. The target domain image generator utilizes the architecture of U-net [34] and creates high-quality generated output by learning to reduce the adversarial loss and the sum of the mean squared error of the generated output and the original input.

After, CycleGAN [42] and DiscoGAN [19] are proposed to translate images between unpaired images. The architecture for both models is the almost same. CycleGAN adopts ResNet [14] as the backbone structure for the network while DiscoGAN does the simple encoder and decoder with multiple convolution networks. They consist of two generators and a discriminator. They make generators learn the inverse function relationship by reconstructing the original images from both reconstructed and generated images. The discriminator is only learned to distinguish whether the target domain is real or fake. The objective function is defined with the the cycle consistency loss for the error between the original reconstructed images and the adversarial loss.

StyleGAN [15] is designed to understand and control image feature space. It generates a latent code that reflects the feature distribution of the image through the mapping network. The generated latent code is applied to each layer in generator through an adaptive instance normalization method. StyleGAN constructs the

feature space entangled through the mapping network and generator can show natural style change and high-quality generated output.

StarGAN [10] translates an image to multi-domain images using a single generator and discriminator. For multi-domain translations, it has the style network that extracts style vectors from each domain. The generator performs multi-domain translation by using the style vector as an conditional input. It was trained by adding the adversarial loss and cycle consistency loss, as well as style loss that the style vector of the restored data should be similar.

### 3 PROPOSED METHOD

#### 3.1 Electrocardiogram

We briefly introduce an ECG which records the electrical signals generated by the heart by using external electrodes. Figure 1 shows an example for a sampled signal in any lead of an ECG, which represents atrial and ventricular depolarization and repolarization using wave points: QRS complex and P/T/U waves.

The standard ECG consists of six limb leads and six precordial leads. The six limb leads record the electrophysiologic changes of the heart in a horizontal plane, while the other six precordial leads record changes in the heart at the axial plane. Various hand-crafted features (e.g., Amplitudes and duration at the waves, PR interval, QT interval, ST segment, TP segment, RR interval, and so on.) are derived from wave points on 12 leads. Conventionally, they are used to analyze cardiac conditions.

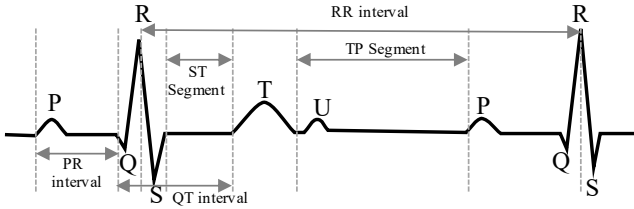


**Figure 1: A sampled signal in a lead of an ECG. It consists P, Q, R, S, T, and U wave points. Various hand-crafted features are derived from wave points such as Amplitudes and duration at the waves, PR interval, QT interval, ST segment, TP segment, RR interval, and so on.**

#### 3.2 Problem Definition

If the loss of some leads in an ECG, this could make a wrong diagnosis. This is because of a limitation in the interpretation of the heart condition due to the loss of spatial information. For example, when the right coronary artery, which supplies blood to the inferior aspect of the heart, is occluded by a blood clot, the inferior leads of the ECG (namely, Lead II, Lead III, and aVF) capture the ST segment deviation. Without the inferior leads, it is difficult to reach a precise diagnosis. Previous studies also reported that the lack of availability of leads using wearable devices might result in a misdiagnosis of acute myocardial infarction [9, 23, 36].

With the appearance of various wearable devices measurable to an ECG, someone enables to check the status of the cardiac

condition immediately anywhere [17, 29, 32, 38]. Though such devices provide ECGs with only a single lead [5], recently, a study reported that she could record asynchronous multiple leads using a wearable device, depending on the different positions of the device.

A lead has a signal projected for the vector representing the magnitude and direction of electrical activity by the cardiomyocytes at any particular axis. Using their vector operations, the other unobserved leads on the same axis are conjectured from at least two leads. Also, we claim that the leads in the orthogonal axis could be inferred if a model understands patterns for the relation between different axes.

We propose a method for the ECG synthesis from two asynchronous leads to ten leads based on GAN, and call this ECGT2T. To the best of our knowledge, there are no reported generative models to construct completely the standard 12-lead ECGs by using only some limited leads. We expect to improve the diagnosis performance of cardiac diseases by constructing the standard 12-lead ECG observed on a global view of the physiological status of the heart.

#### 3.3 Framework

Figure 2 shows the architecture of ECGT2T. This model consists of four networks: style, mapping, generative, and discriminative networks. Each component named *block* in networks is implemented by multiple basic residual blocks [14].

ECGT2T works following the concept of image-to-image translation models which translate a source image to a target image with the desired style of the reference image [10, 26, 42]. ECGT2T first encodes the cardiac condition from two given leads. Referring to the cardiac condition, it represents ten lead styles for corresponding leads. Finally, it generates the unobserved lead using a single input lead with a desired lead style. Let  $x_i \in X$  be any lead of the 12-lead ECG, where  $i$  ranges from Lead I to V6. The roles of the networks are as follows.

**Style network  $S(\cdot)$**  It represents the cardiac styles  $c_{x_i} \in C$  for ten respective leads from given two leads ( $c_{x_i} = S(x_{I,II}, i)$ ). It first encodes  $c_{x_I}$  and  $c_{x_{II}}$  by style encoding blocks, and extract the latent code  $c_{x_{I\&II}}$  implying the heart condition from one concatenated with two styles by dual reference encoding blocks. Finally, the latent code is transformed to  $c_{x_i}$  by the corresponding style encoding block. These cardiac styles are used for the style translation at the generate network  $G(\cdot)$ .

**Mapping network  $M(\cdot)$**  It is devised in [10, 18] for the efficient style translation. We adopt another network to represent the cardiac styles  $\tilde{c}_{x_i} \in \tilde{C}$  for ten respective leads from a random variable  $z \in Z$ , instead of two given leads ( $\tilde{c}_{x_i} = M(z, i)$ ). It represents the latent code using the multi-layer perceptron, and then conditionally generate  $\tilde{c}_{x_i}$  on the corresponding style encoding block. This network makes style network  $S(\cdot)$  to be robust by influencing generated styles.

**Generative network  $G(\cdot)$**  It generates a single base input lead  $x_i$  to the desired lead  $\tilde{x}_i$  using the desired cardiac style  $c_i$ , ( $\tilde{x}_i = G(x_i, c_i)$ ). The input encoding block represents a latent code from  $x_i$  and the decoding block reconstructs  $\tilde{x}_i$  injecting  $c_i$  represented from style network  $S(\cdot)$  via the adaptive instance normalization [15] that efficiently transforms the style.

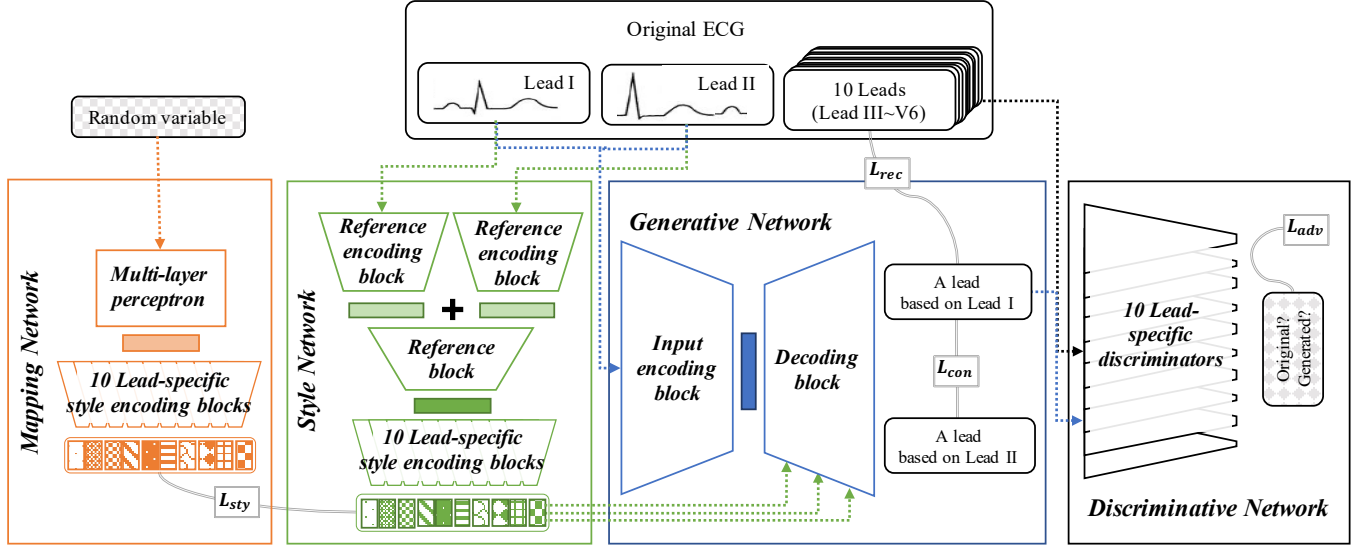


Figure 2: The ECGT2T architecture. There are style, mapping, generative, and discriminative networks. In each network, the block component consists of multiple basic residual blocks [14]. The style network represents the cardiac styles for ten respective leads from the given two leads. The mapping network is another network to represent the cardiac styles from a random variable. The generative network generates a single base input lead to the desired lead using the desired cardiac style. The discriminative network distinguishes whether its input is real or not.  $L$  indicates a loss function.

**Discriminative network**  $D(\cdot)$  It is the network typically used in GAN [28] which distinguishes whether its inputs are real or not ( $y = D(x_i, x_i)$ ). It is composed to multiple discriminators as many as the number of leads to be generated.

### 3.4 Objectives

Our framework includes four objectives as follows.

**Adversarial objective** We use the typical adversarial loss in a GAN. This is formulated by the average of the log probability for original leads and the log of the inverted probabilities of the generated ones. The equation is expressed as follows:

$$L_{adv} = \mathbb{E}[\log D(x_i)] + \mathbb{E}[\log(1 - D(G(x_I, c_i)))],$$

where  $i$  is randomly selected from Lead III to V6, in practical.

**Reconstruction** To construct realistic leads from  $G$ , we define the equation comparing the original and generated leads as follows:

$$L_{rec} = \mathbb{E}[(x_j - G(x_i, c_j))^2],$$

where  $i$  is alternatively chosen as Lead I or Lead II while  $j$  is randomly selected from Lead III to V6, in practical. Peaks in an ECG (e.g., Q, R, and S wave points) could be shown as outliers in the graphical perspective. Since such peaks are practically used as the import decision point to diagnose heart diseases, an accurate depiction is required. Thus we used the mean squared error that is more sensitive to outliers.

**Lead consistency** Given two asynchronous leads, we have an option as a base input lead. We hope that outputs must be equal by a given cardiac style, even if base input leads are different. To maintain such consistency among generated leads regardless of any base leads, we define the objective for the lead consistency as

follows:

$$L_{con} = \mathbb{E}[(G(x_I, c_i) - G(x_{II}, c_i))^2],$$

where  $i$  is randomly selected from Lead III to V6. To gauge the discrepancy for leads, we also used the mean squared error.

**Style consistency** Since subjects have different heart conditions and body shapes, the cardiac rhythm and beat shapes in leads are very diverse. Therefore, Style network  $S(\cdot)$  avoids deriving a biased style. This objective prevents overfitting and helps regularization by using the discrepancy between styles derived from style network  $S(\cdot)$  and mapping network  $M(\cdot)$ .

$$L_{sty} = \mathbb{E}[|(M(z, i) - S(x_{I,II}, i))|_1],$$

where  $z$  is a random variable and  $i$  is randomly selected from Lead III to V6. When computing the difference for styles, we adopt the mean absolute error, instead of the mean squared error.

**Full objective** the full objective is summarized as follows.

$$\min_{E,H,G} \max_D = \lambda_{adv} L_{adv} + \lambda_{rec} L_{rec} + \lambda_{con} L_{con} + \lambda_{sty} L_{sty}$$

where all  $\lambda$ s are the hyperparameters for each term.

## 4 EXPERIMENTS

This section evaluates 1) synthetic quality and 2) availability as a lead augmentation for ECGT2T. For the synthetic quality assessment, we compared the features between original and generated leads. For the availability, we first augmented insufficient leads and construct the standard 12-lead ECG set. We then compared the performance of deep learning models using original and generated ECGs on the cardiac disease classifications.

## 4.1 Experimental setup

**4.1.1 Dataset.** Table 1 lists the datasets used in our experiments, which denotes the number of ECG samples and the proportion of event samples for cardiac diseases. We obtained both a large publicly available ECG dataset collected at the Physikalisch-Technische Bundesanstalt (PTB-XL) [37] and an ECG dataset collected at Chapman University and Shaoxing People’s Hospital (CUSPH) [40].

**Table 1: ECG Dataset**

Dataset	#total	#train	#validation	#test	Abnormal proportion
PTB-XL	15,012	10,508	1,501	3,003	36.6%
CUSPH	9,094	6,365	910	1,819	19.6%

The PTB-XL dataset provides ECGs with multiple diagnostic statements. This is composed of 21,837 standard 12-lead ECGs, each of which has 10 seconds length with a sampling rate of 500Hz. We only selected 15,012 ECGs with 9,527 normal ECG samples and 5,485 ECG samples labeled by any myocardial infarction, respectively. CUSPH provides 10,646 ECGs with diverse types of arrhythmia, each of which consists of 12 leads taken over a period of 10 seconds with a 500 Hz sampling rate. For cardiac rhythms, we selected ECG samples for 7,314 normal and 1,780 atrial fibrillation samples. Both datasets were split into training, validation, and test with a ratio of 7:1:2. Train, validation, and test datasets have the same distribution for normal and cardiac disease ECG samples. As the pre-processing, we only cropped ECGs to about four seconds to reduce the training time and conduct the z-score normalization for all leads. For two asynchronous leads, we first sampled a signal in Lead I and then selected the delayed signal to 0.5 seconds in Lead II. For an instance, while a signal is sampled ranging from one to 5 seconds for Lead I, another one is extracted ranging from 1.5 to 5.5 seconds for Lead II.

**4.1.2 Model.** For hyper-parameters of *ECGT2T*, we set the size of all intermediate vector to 512. The Adam optimization [20] is used with the learning rate of style, mapping, generative, and discriminative networks with  $3e^{-4}$ ,  $1e^{-4}$ ,  $3e^{-4}$ , and  $1e^{-4}$ , respectively, and the weight decay for all networks  $1e^{-4}$ .  $\lambda_{rec}$  is set to 2, while the others are set to 1.

To evaluate how realistic 12-lead ECG sets constructed by *ECGT2T* are, we developed another generative model for ECG synthesis from single to 11 leads (*ECGS2E*). There are the following differences. The mapping and style networks in *ECGS2E* consist of 11 lead-specific style encoding blocks. Because the base input is only a single lead, single reference encoding block in the style network instead of two ones on that in *ECGT2T*. Also,  $L_{con}$  of objectives is absent. Its hyper-parameters are the same as those of *ECGT2T*. Under this setting, we took seven days to train two generative models (*ECGT2T* and *ECGS2E*) on the PTB-XL training set.

We also demonstrated them as a lead augmentation method in the classification tasks. We implemented a classifier based on ResNet18 [14] that adopts residual blocks with one-dimensional convolution networks and embeds a single fully connected layer in the last layer. The focal loss [25] is used with  $\alpha$  and  $\gamma$  set to 0.5 and

2, respectively and the Adam optimization [20] is used with the learning rate and weight decay set to  $1e^{-4}$  and  $1e^{-5}$  respectively.

All our models are implemented on the PyTorch framework and executed on a server equipped with Intel Xeon Silver 4210, 256 GB memory, and four GEFORCE RTX 3090 with 24 GB memory.

**Table 2: Synthetic quality assessment for both amplitude magnitude and arrangement for the R-peak on generated leads**

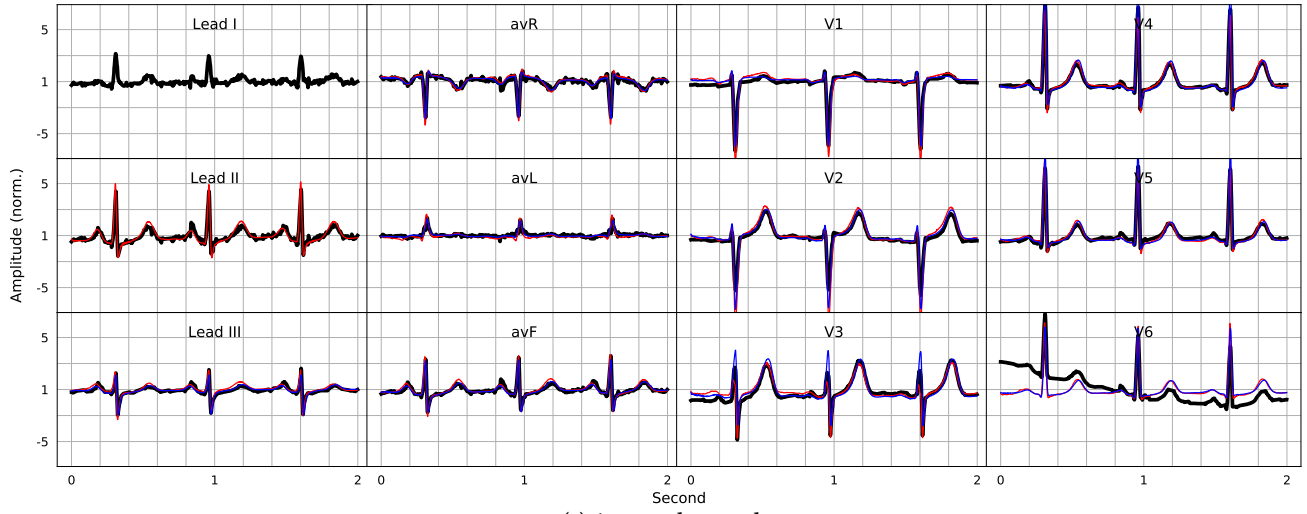
Dataset	Lead	V1		V5	
	Model	ECGT2T	ECGS2E	ECGT2T	ECGS2E
PTB-XL	Amp	6.4%	6.4%	7.3%	6.7%
	Pos	8.3ms	8.2ms	2.0ms	2.2ms
CUSPH	Amp	11.4%	11.2%	7.6%	7.7%
	Pos	12.9ms	14.4ms	3.8ms	4.1ms

## 4.2 ECG generation

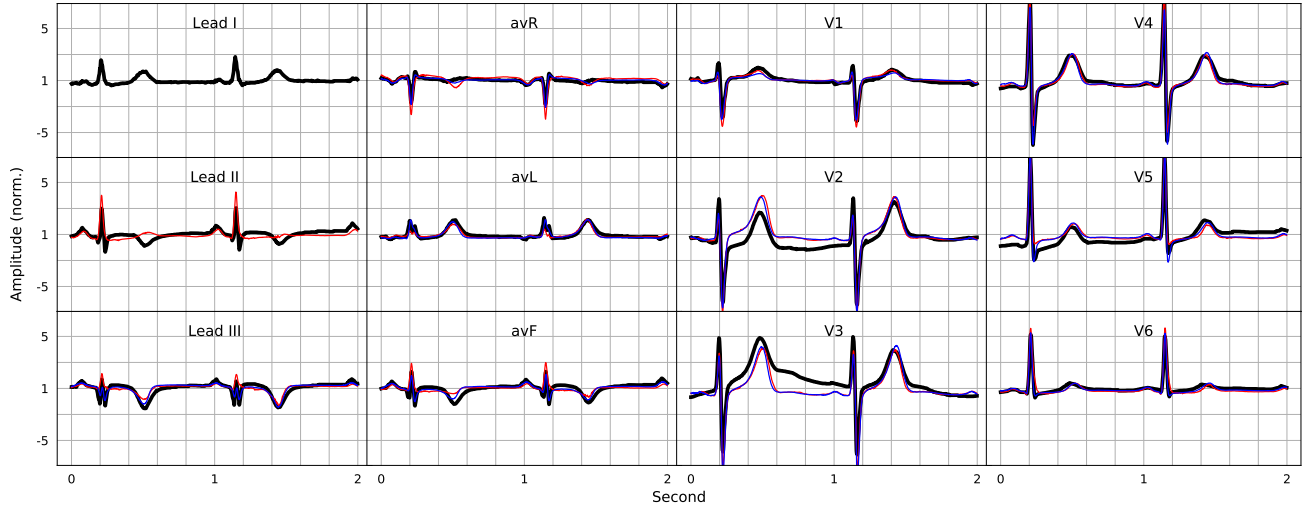
Though there are diverse measurements [2] to compare the discrepancy between signals such as percent root mean square difference, root mean square error, and Fréchet distance, they are not suitable to reflect the synthetic quality of generated ECGs. If only some leads in an original ECG have some artifacts such as the power line interference, myokymia, and baseline wandering, the well-generated ECGs with ignoring such artifacts could be undervalued.

Thus, we conducted the synthetic quality assessment by comparing wave points between original and generated ECGs. There are various wave points called P, Q, R, S, T, and U. Some peaks in an ECG by a subject with cardiac diseases could not be detected while the R-peak is almost detected. Also, the R-peak is one of the most important points to which the features related are used for diagnosing the heart conditions such as the heart rate and the level of stress [35]. We measured the magnitude gap of amplitude and positional missing error for the R-peak. In twelve leads, we chose two leads (V1 and V5) measured at distinctly different locations. Over the base Lead I, V1 is recorded in orthogonal position while V5 is recorded in similar positions. To measure the difference for the R-peak, we first generated the leads for V1 and V5 from *ECGT2T* and *ECGS2E*. Then, we found R-peak using Neurokit2 [27], the popular Python Toolbox for Neurophysiological Signal Processing library, on original generated V1 and V5, respectively.

Table 2 shows the magnitude gap of the amplitude (*Amp*) and the position missing error (*Pos*) for the V1 and V5 generated by *ECGT2T* and *ECGS2E* on each dataset, respectively. In the PTB-XL dataset, we found the magnitude gap ranging only 6~7% and the positional missing under 10 ms. In the CUSPH dataset, not used in the training phase, we found the results are a bit larger than those in the PTB-XL dataset, but the tendency is similar. There are commonly more positional missing errors at V1 over V5. These results seem that the synthetic performance of *ECGS2E* is a little better than that of *ECGT2T*. In addition, it seems to have somewhat distinct amplitude errors. However, we claim that these errors are ignored via visual outcomes following figures.



(a) A normal example



(b) A myocardial infarction example

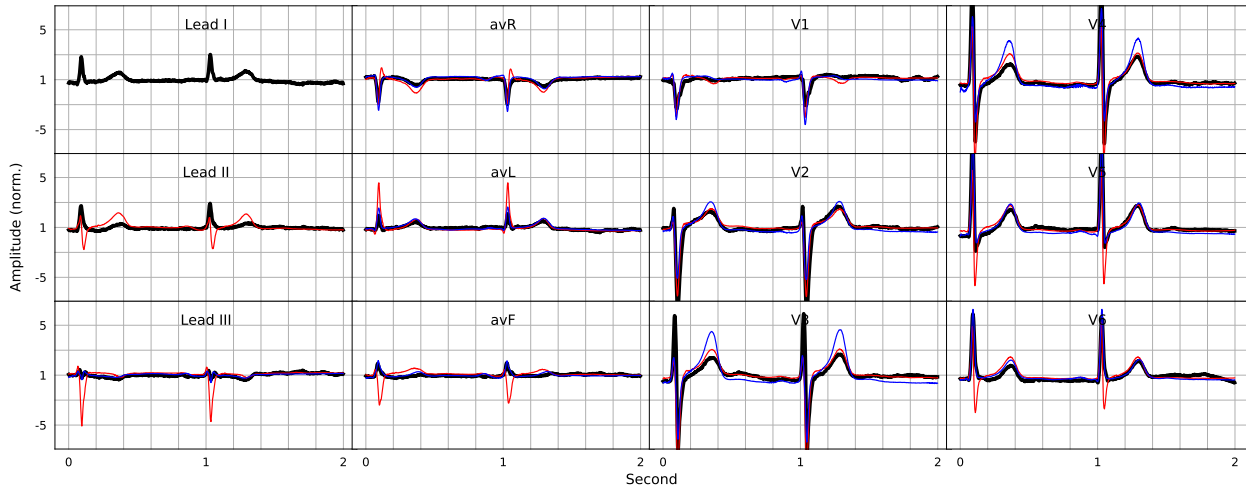
**Figure 3: Examples for the 12-lead ECG with the normal and myocardial infarction in the PTB-XL dataset, respectively. The lines with black, blue, and red colors indicates signals by original, ECGT2T, and ECGS2E, respectively. ECGS2E displays 11 leads because it is trained using only Lead I, while ECGT2T using asynchronous Lead I& Lead II draws signals for 10 leads. For convenience, all leads are illustrated synchronously, although ECGT2T uses two asynchronous leads. Each lead represents the amplitude changes of the signal over about 2 seconds.**

Figure 3 shows ECG examples in the PTB-XL dataset where the black, red, and blue lines indicate the signals for the original, ECGS2E, and ECGT2T, respectively. For brevity's sake, we additionally cropped the 12-lead ECGs about 2 seconds from 4-second signals. Each lead shows the amplitude changes over time. ECGS2E synthesizes 11 leads because it is trained using only Lead I, while ECGT2T using asynchronous Lead I& Lead II generates 10 leads. For convenience, all leads are illustrated synchronously, although ECGT2T uses two asynchronous leads.

Figure 3a is a 12-lead ECG for the normal example. As expected, in all leads, the amplitudes changes over seconds are similar. In particular, ten leads generated by ECGT2T are nearly equivalent to the original ones. Interestingly, the leads of ECGS2E, including even Lead II, resemble the original ones. In addition, we note that there are effects for the removal of noise (e.g., aVR and aVL) and baseline wandering (e.g., V1, V3, and V6) by generative models. Such corrections cause the amplitude gaps between original and generated ones.



(a) A normal example



(b) A atrial fibrillation example

**Figure 4: Examples for the 12-lead ECG on the normal and atrial fibrillation in the CUSPH dataset, respectively. The lines with black, blue, and red colors indicates signals by original, ECGT2T, and ECGS1E, respectively. ECGS2E displays 11 leads because it is trained using only Lead I, while ECGT2T using asynchronous Lead I& Lead II draws signals for 10 leads. For convenience, all leads are illustrated synchronously, although ECGT2T uses two asynchronous leads. Each lead represents the amplitude changes of the signal over about 2 seconds.**

Figure 3b shows a 12-lead ECG example for the subject with the myocardial infarction, where blood flow to a particular part of the heart decreases or ceases completely. ECGs with myocardial infarction have some characteristics such as the ST-segment elevation, T-wave inversion, and abnormal Q waves at some leads [31]. We observed such signs at Lead II, Lead III, V2, and V3. In typically normal ECGs, Lead I and Lead II have toward the same direction for the peak amplitude at the wave points. ECGS2E referring to Lead I eventually outputs the positive amplitude for the T-wave like that of Lead I. In other words, ECGS2E has no choice but to miss the unexpected inverse T-wave in Lead II. On the other hand, ECGT2T is less relatively affected and generates the ECG similar

to the original one because it recognizes the electrical pathophysiology of the heart more accurately using two vector signals. Both models calibrate the ST-segment elevation at the first beat in V3. Such abnormal examples cause the side-effect for the correction of the baseline at exceptional shapes.

We showed another example for the CUSPH dataset with different type of the cardiac disease as not used in the training phase as shown in Figure 4. All expressions of results is common to Figure 3. Figure 4a shows the normal example. Though there are some magnitude errors of amplitude at ECGS2E, all models well draw all wave points in signals as the normal example in the PTB-XL dataset



(i.e., Figure 3a). In addition, signals in some leads are corrected (e.g., V4~6)

Figure 4b shows an ECG for a subject with atrial fibrillation, which is characterized by the absence of the P-wave, irregularly irregular ventricular rate, and slightly aberrant QRS complexes [30]. Such abnormal features are typically observed in all leads. In this example with absence of the P-wave in all leads, both ECGT2T and ECGS2E output the signals without the P-wave in all leads. As the result of ECGS2E in Figure 3b, the amplitude magnitude of peaks on ECGS2E strays from the original one though the arrangement of wave points are well matched. Since arrhythmia is relevant to the abnormal wave points, the errors of the amplitude magnitude for the peaks in leads could not affect to find the arrhythmia cases.

In the conclusion for the ECG generation, we identified, in the normal examples, both models draw exquisitely other leads compared with original ones, besides V1 and V5 which are used in the quality assessment. They also have the effect of correction to the artifacts. There are some limitations on the examples with heart diseases. For the purpose of correcting the outputs, the models transform the shape of wave points that can be important clues to determine classes. The error of the amplitude magnitude on case examples is larger than that on normal examples. Finally, as we claimed, the generation performance of ECGT2T referring to two leads outperforms that of ECGS2E using a single lead. For the applicability, we tried to use ECGT2T as the lead augmentation method in the following section.

### 4.3 ECG classification

We used ECGT2T as the lead augmentation method for the improvement of the ECG classification performance. For the performance comparison, we configured six evaluation ECG sets with different lead combinations: *Single* means the ECG set composed with only Lead I. *SyncTwo* and *AsyncTwo* denote ECG sets composed of both synchronous and asynchronous Lead I & Lead II, respectively. *S2E* signifies the 12-lead ECG set with original Lead I and other generated leads while *T2T* does the 12-lead ECG set with original Lead I & Lead II and other generated leads. *Original* is the baseline 12-lead ECG set fully constructed by the original.

We train and test six classifiers for the corresponding ECG sets, respectively. As evaluation metrics, we used the area under the receiver operating characteristic curve (AUROC) with 95% confidence interval(CI) and the area under the precision-recall curve (AUPRC) with 95% CI.

Figure 5 shows the performance of the classification for myocardial infarction on the PTB-XL dataset. The result shows that the classifier using *T2T* outperforms the other models, except for the classifier using *Original*. However, the performance of the classifier using *S2E* is worse than those of the models using two leads (i.e., *SyncTwo* and *AsyncTwo*). In particular, the classifier using *Single* shows the worst performance since it misses the diagnosable signs for myocardial infarction. Because myocardial infarction is caused by ischemic necrosis of the myocardium supplied by the occluded coronary artery, a 12-lead ECG is required to diagnose the particular type of myocardial infarction, effectively to narrow down to the distribution of the exactly blocked vessel. In other words, the myocardial infarction can not be diagnosed precisely without all

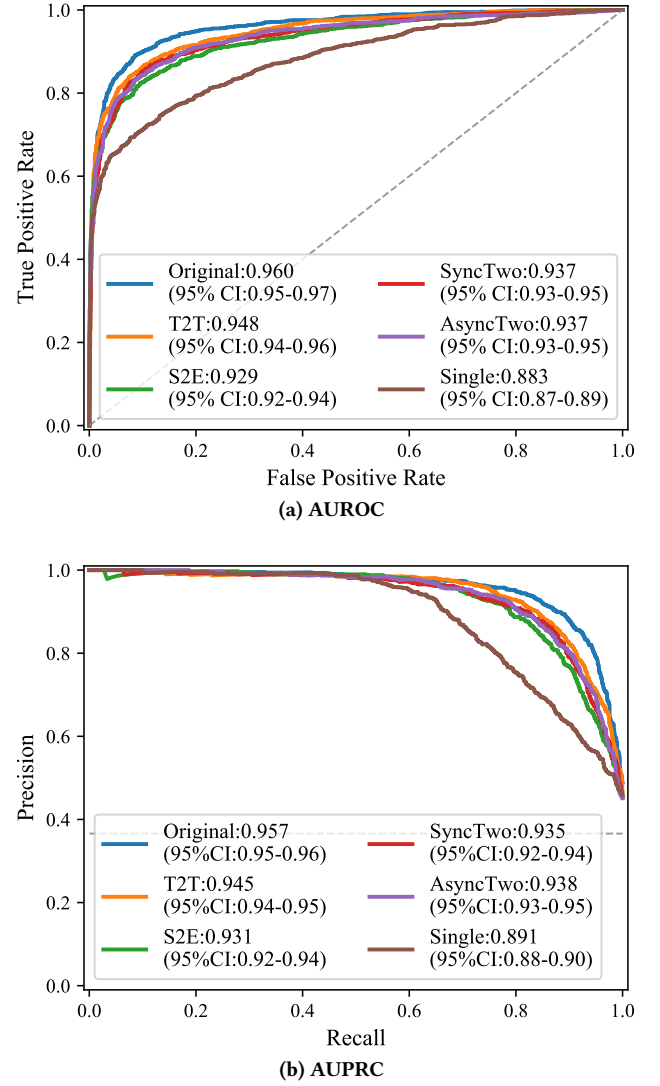


**Figure 5: Classification performance for myocardial infarction on the PTB-XL dataset.**

the leads affected by each sub-type of infarction: right coronary artery leads (i.e., Lead II, Lead III, and aVF), left anterior descending artery leads (i.e., V1-V4), and left circumflex artery (i.e., V5-V6, Lead I, and aVL), named to inferior infarction, anteromedial infarction, and anterolateral infarction, respectively. Therefore, we identified that ECGs with partial leads cause misdiagnosis.

Figure 6 shows the classification performance for the atrial fibrillation on the CUSPH dataset. Overall, the classifiers trained by lead augmented sets outperform others, except for *Original*. However, there are only few performance differences between classifiers on the CUSPH dataset, compared to that on the PTB-XL dataset. Interestingly, the classifier using *S2E* is subtly ahead of that trained by *T2T* on both metrics. On the AUROC metric, the classifier trained by *Single* is slightly better than that trained by *AsyncTwo*.



Unlike myocardial infarction detected by the shape change of the beat, such arrhythmia can be diagnosed if there are irregularly irregular rhythmic patterns in a lead. In other words, it is not required for use of whole 12 leads to detect the abnormal rhythm. Therefore, we found a narrow gap of classifier performances for the arrhythmia classification.

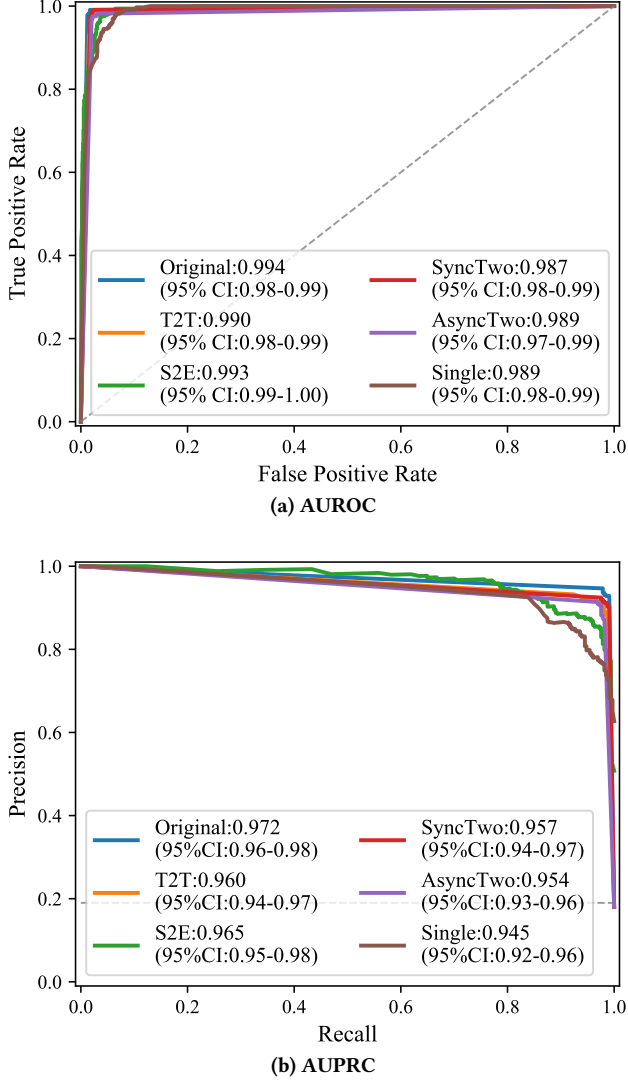


**Figure 6: Classification performance for arrhythmia on the CUSPH dataset.**

## 5 CONCLUSION

An ECG is a painless and non-invasive tool for diagnosing cardiac diseases. It records the electrical signals from different directions using 12 leads. Recent wearable devices such as smartwatches provide a facility to measure ECG with a couple of leads. However, such an ECG with partial leads can result in an inaccurate diagnosis of cardiac disease.

A lead has a signal projected for the vector representing the magnitude and direction of electrical activity at any particular axis. The vector operations using some leads actually enable to conjecture other unobserved leads.

With adopting such a mechanism, we propose the deep generative model based on GAN for the ECG synthesis from two asynchronous leads to ten leads, so-called ECGT2T. This model generates a desired lead from a given single base lead with the desired lead style. It consists of four networks. The style network first encodes a latent code representing the cardiac condition from two asynchronous leads. It then represents the cardiac style code for the corresponding lead. The mapping network also encodes ten styles from a random variable. Its role is to enhance the representation capacity encoding styles in the style network. The generative network produces a target lead. The discriminative network distinguishes whether the given leads are real or not.

We first measured how sophisticatedly the model generate leads. To this end, we examine the R-peaks, an important wave point, in generated leads. there are errors for the magnitude gap of amplitude about 10% and delayed arrangement within 15ms. We claim that these errors do not have a significant effect. To verify such claims, we checked outputs in detail.

On the normal examples, ECGT2T constructs the standard 12-lead ECG almost identical to the original, even it shows the correction effect removing noise and baseline wandering, causing errors in diagnosis. In the case of abnormal examples such as myocardial infarction and atrial fibrillation, ECGT2T generates almost the same leads compared with the original. However, its ability to the correction work as a side-effect. It sometimes causes to change from the sign to detect cardiac disease to normal sign.

We also used our model as a lead augmentation method. On the PTB-XL dataset, the classifier trained the 12-lead ECG by ECGT2T outperforms others using ECG sets with only limited leads. On the CUSPH dataset, the classifier using the 12-lead ECG by ECGT2T also shows the excellent performance that was comparable to the classifier using the standard 12-lead ECGs. This results show that ECGT2T improves the performance of the classification model by constructing the realistic 12-lead ECG using only two asynchronous leads.

With the rapid dissemination of many smartwatches, we expect that ECGT2T provides to correct measurement errors in ECGs and helps detect abnormalities of the heart earlier. For future work, we will devise a way to solve side effects for the baseline correction and will develop and improve the model that constructs the more sophisticated 12-lead ECG using only a single lead.

## REFERENCES

- [1] U Rajendra Acharya, Hamido Fujita, Shu Lih Oh, Yuki Hagiwara, Jen Hong Tan, and Muhammad Adam. 2017. Application of deep convolutional neural network for automated detection of myocardial infarction using ECG signals. *Information Sciences* 415 (2017), 190–198.
- [2] Mohammed AlMahamdy and H Bryan Riley. 2014. Performance study of different denoising methods for ECG signals. *Procedia Computer Science* 37 (2014), 325–332.
- [3] Karol Antczak. 2020. A Generative Adversarial Approach To ECG Synthesis And Denoising. *arXiv preprint arXiv:2009.02700* (2020).
- [4] Zachi I Attia, Peter A Noseworthy, Francisco Lopez-Jimenez, Samuel J Asirvatham, Abhishek J Deshmukh, Bernard J Gersh, Rickey E Carter, Xiaoxi Yao, Alejandro A Rabinstein, Brad J Erickson, et al. 2019. An artificial intelligence-enabled ECG algorithm for the identification of patients with atrial fibrillation during sinus rhythm: a retrospective analysis of outcome prediction. *The Lancet* 394, 10201

- (2019), 861–867.
- [5] Cesar O Avila. 2019. Novel use of Apple Watch 4 to obtain 3-lead electrocardiogram and detect cardiac ischemia. *The Permanente Journal* 23 (2019).
  - [6] Ulas Baran Baloglu, Muhammed Talo, Ozal Yildirim, Ru San Tan, and U Rajendra Acharya. 2019. Classification of myocardial infarction with multi-lead ECG signals and deep CNN. *Pattern Recognition Letters* 122 (2019), 23–30.
  - [7] Manuel Blanco-Velasco, Binwei Weng, and Kenneth E Barner. 2008. ECG signal denoising and baseline wander correction based on the empirical mode decomposition. *Computers in biology and medicine* 38, 1 (2008), 1–13.
  - [8] Eoin Brophy. 2020. Synthesis of Dependent Multichannel ECG using Generative Adversarial Networks. In *Proceedings of the 29th ACM International Conference on Information & Knowledge Management*. 3229–3232.
  - [9] Younghoon Cho, Joon-myoung Kwon, Kyung-Hee Kim, Jose R Medina-Inojosa, Ki-Hyun Jeon, Soohyun Cho, Soo Youn Lee, Jinsik Park, and Byung-Hee Oh. 2020. Artificial intelligence algorithm for detecting myocardial infarction using six-lead electrocardiography. *Scientific reports* 10, 1 (2020), 1–10.
  - [10] Yunjei Choi, Youngjung Uh, Jaeyun Yoo, and Jung-Woo Ha. 2020. Stargan v2: Diverse image synthesis for multiple domains. In *Proceedings of the IEEE/CVF Conference on Computer Vision and Pattern Recognition*. 8188–8197.
  - [11] Anne Marie Delaney, Eoin Brophy, and Tomas E Ward. 2019. Synthesis of realistic ecg using generative adversarial networks. *arXiv preprint arXiv:1909.09150* (2019).
  - [12] Tomer Golany and Kira Radinsky. 2019. Pgens: Personalized generative adversarial networks for ecg synthesis to improve patient-specific deep ecg classification. In *Proceedings of the AAAI Conference on Artificial Intelligence*, Vol. 33. 557–564.
  - [13] Awni Y Hannun, Pranav Rajpurkar, Masoumeh Haghpanahi, Geoffrey H Tison, Codie Bourn, Mintu P Turakhia, and Andrew Y Ng. 2019. Cardiologist-level arrhythmia detection and classification in ambulatory electrocardiograms using a deep neural network. *Nature medicine* 25, 1 (2019), 65–69.
  - [14] Kaiming He, Xiangyu Zhang, Shaoqing Ren, and Jian Sun. 2016. Deep residual learning for image recognition. In *Proceedings of the IEEE conference on computer vision and pattern recognition*. 770–778.
  - [15] Xun Huang and Serge Belongie. 2017. Arbitrary style transfer in real-time with adaptive instance normalization. In *Proceedings of the IEEE International Conference on Computer Vision*. 1501–1510.
  - [16] Phillip Isola, Jun-Yan Zhu, Tinghui Zhou, and Alexei A Efros. 2017. Image-to-image translation with conditional adversarial networks. In *Proceedings of the IEEE conference on computer vision and pattern recognition*. 1125–1134.
  - [17] AliveCor KardiaMobile. 2021. <https://clinicians.alivecor.com/our-devices/>.
  - [18] Tero Karras, Samuli Laine, and Timo Aila. 2019. A style-based generator architecture for generative adversarial networks. In *Proceedings of the IEEE/CVF Conference on Computer Vision and Pattern Recognition*. 4401–4410.
  - [19] Taeksoo Kim, Moonsu Cha, Hyunsoo Kim, Jung Kwon Lee, and Jiwon Kim. 2017. Learning to discover cross-domain relations with generative adversarial networks. In *International Conference on Machine Learning*. PMLR, 1857–1865.
  - [20] Diederik P Kingma and Jimmy Ba. 2014. Adam: A method for stochastic optimization. *arXiv preprint arXiv:1412.6980* (2014).
  - [21] Hanno U Klemm, Rodolfo Ventura, Thomas Rostock, Benedikt Brandstrup, Tim Ritsius, Thomas Meinertz, and Stephan Willems. 2006. Correlation of symptoms to ECG diagnosis following atrial fibrillation ablation. *Journal of cardiovascular electrophysiology* 17, 2 (2006), 146–150.
  - [22] Wei-Yin Ko, Konstantinos C Siontis, Zachary I Attia, Rickey E Carter, Suraj Kapa, Steve R Ommen, Steven J Demuth, Michael J Ackerman, Bernard J Gersh, Adelaide M Arruda-Olson, et al. 2020. Detection of hypertrophic cardiomyopathy using a convolutional neural network-enabled electrocardiogram. *Journal of the American College of Cardiology* 75, 7 (2020), 722–733.
  - [23] Vessela Krasteva, Irena Jekova, and Roger Abächerli. 2017. Biometric verification by cross-correlation analysis of 12-lead ECG patterns: Ranking of the most reliable peripheral and chest leads. *Journal of electrocardiology* 50, 6 (2017), 847–854.
  - [24] Joon-myoung Kwon, Kyung-Hee Kim, Howard J Eisen, Younghoon Cho, Ki-Hyun Jeon, Soo Youn Lee, Jinsik Park, and Byung-Hee Oh. 2020. Artificial intelligence assessment for early detection of heart failure with preserved ejection fraction based on electrocardiographic features. *European Heart Journal-Digital Health* (2020).
  - [25] Tsung-Yi Lin, Priya Goyal, Ross Girshick, Kaiming He, and Piotr Dollár. 2017. Focal loss for dense object detection. In *Proceedings of the IEEE international conference on computer vision*. 2980–2988.
  - [26] Ming-Yu Liu, Thomas Breuel, and Jan Kautz. 2017. Unsupervised image-to-image translation networks. *arXiv preprint arXiv:1703.00848* (2017).
  - [27] Dominique Makowski, Tam Pham, Zen J. Lau, Jan C. Brammer, François Lespinasse, Hung Pham, Christopher Schölzel, and S. H. Annabel Chen. 2021. NeuroKit2: A Python toolbox for neurophysiological signal processing. *Behavior Research Methods* (02 Feb 2021). <https://doi.org/10.3758/s13428-020-01516-y>
  - [28] Mehdi Mirza and Simon Osindero. 2014. Conditional generative adversarial nets. *arXiv preprint arXiv:1411.1784* (2014).
  - [29] Beurer mobile ECG device. 2021. <https://www.beurer.com/web/gb/products/medical/ecg-and-pulse-oximeter/mobile-ecg-device/>.
  - [30] Brian Olshansky, Mina K Chung, Steven M Pogwizd, and Nora Goldschlager. 2016. *Arrhythmia Essentials E-Book*. Elsevier Health Sciences.
  - [31] Akbar A Panju, Brenda R Hemmelgarn, Gordon H Guyatt, and David L Simel. 1998. Is this patient having a myocardial infarction? *Jama* 280, 14 (1998), 1256–1263.
  - [32] PocketECG. 2021. <https://www.pocketecg.com/pocketecg>.
  - [33] Donald W Romhilt and E Harvey Estes Jr. 1968. A point-score system for the ECG diagnosis of left ventricular hypertrophy. *American heart journal* 75, 6 (1968), 752–758.
  - [34] Olaf Ronneberger, Philipp Fischer, and Thomas Brox. 2015. U-net: Convolutional networks for biomedical image segmentation. In *International Conference on Medical image computing and computer-assisted intervention*. Springer, 234–241.
  - [35] Deboleena Sadhukhan and Madhuchhanda Mitra. 2012. R-peak detection algorithm for ECG using double difference and RR interval processing. *Procedia Technology* 4 (2012), 873–877.
  - [36] Carmen Anna Maria Spaccarotella, Alberto Polimeni, Serena Migliarino, Elisa Principe, Antonio Curcio, Annalisa Mongiardo, Sabato Sorrentino, Salvatore De Rosa, and Ciro Indolfi. 2020. Multichannel electrocardiograms obtained by a Smartwatch for the diagnosis of ST-segment changes. *JAMA cardiology* 5, 10 (2020), 1176–1180.
  - [37] Patrick Wagner, Nils Strodthoff, Ralf-Dieter Boussejot, Dieter Kreiseler, Fatima I Lunze, Wojciech Samek, and Tobias Schaeffter. 2020. PTB-XL, a large publicly available electrocardiography dataset. *Scientific data* 7, 1 (2020), 1–15.
  - [38] Galaxy Watch. 2021. <https://www.samsung.com/us/mobile/wearables/all-wearables/>.
  - [39] Naren Wulan, Wei Wang, Pengzhong Sun, Kuanquan Wang, Yong Xia, and Henggui Zhang. 2020. Generating electrocardiogram signals by deep learning. *Neurocomputing* 404 (2020), 122–136.
  - [40] Jianwei Zheng, Jianming Zhang, Sidi Danioko, Hai Yao, Hangyuan Guo, and Cyril Rakovski. 2020. A 12-lead electrocardiogram database for arrhythmia research covering more than 10,000 patients. *Scientific data* 7, 1 (2020), 1–8.
  - [41] Fei Zhu, Fei Ye, Yuchen Fu, Quan Liu, and Bairong Shen. 2019. Electrocardiogram generation with a bidirectional LSTM-CNN generative adversarial network. *Scientific reports* 9, 1 (2019), 1–11.
  - [42] Jun-Yan Zhu, Taesung Park, Phillip Isola, and Alexei A Efros. 2017. Unpaired image-to-image translation using cycle-consistent adversarial networks. In *Proceedings of the IEEE international conference on computer vision*. 2223–2232.